J Paleolimnol (2014) 51:161–177
DOI 10.1007/s10933-012-9662-x

ORIGINAL PAPER

Late Quaternary Qaidam lake histories and implications for an MIS 3 "Greatest Lakes" period in northwest China

David B. Madsen · ZhongPing Lai · YongJuan Sun · David Rhode · XiangJun Liu · P. Jeffrey Brantingham

Received: 20 February 2012 / Accepted: 4 November 2012 / Published online: 27 March 2013
© Springer Science+Business Media Dordrecht 2013

Abstract Da Qaidam and Xiao Qaidam are two of a number of lakes in northwestern China whose lake histories have been used to support the notion of a "Greatest Lakes" period in the region during marine isotope stage (MIS) 3. Reappraisal of the basins' geomorphology, however, suggests that both lakes are highly problematic proxies for past climate. Xiao Qaidam has a low overflow threshold, only ~10–12 m above the lake surface, well below previously estimated high stands, and until about 17–23 ka BP Da Qaidam was occasionally fed by a river whose flow into the lake basin was geomorphically, rather than climatically controlled. Based on limited optically stimulated luminescence dating of shoreline and alluvial sediments it appears that highstands in the basins occurred ~100 ka BP or earlier. The two lakes are thus part of an increasing number of lake records that suggest, at least in northwestern China, (1) some lake histories may not record climate events, and (2) that the "Greatest Lakes" high stands occurred much earlier than previously recognized.

Keywords Qaidam Lakes · Shoreline chronologies · MIS 3 · Late Quaternary · Northwest China

Introduction

Da Qaidam and Xiao Qaidam are small, saline lakes that lie on the northeastern margin of the Qaidam Basin in China's northwestern desert region (Fig. 1). The Qaidam Basin was filled with a series of mega-lake systems during the Pliocene and early-mid Pleistocene (Huang et al. 1993; Wei and Jiang 1994; Mischke et al. 2010), but continued uplift of the Himalayas and Tibetan Plateau during the Cenozoic has gradually starved the region of precipitation (An et al. 2001; Yin et al. 2008). The basin's drainages

D. B. Madsen (✉)
MOE Key Laboratory of West China's Environmental System, Research School of Arid Environment and Climate Change, Lanzhou University, Lanzhou 730000, China
e-mail: dmadsen@austin.rr.com; madsend@mail.utexas.edu

Z. Lai
State Key Laboratory of Cryosphere Sciences, Cold and Arid Regions Environmental and Engineering Research Institute, Chinese Academy of Sciences, Lanzhou 730000, China

Z. Lai · Y. Sun · X. Liu
Luminescence Dating Group, Qinghai Institute of Salt Lakes, Chinese Academy of Sciences, Xining 810008, China

D. Rhode
Earth and Ecosystem Sciences, Desert Research Institute, Reno, NV 89512, USA

P. Jeffrey Brantingham
Department of Anthropology, University of California Los Angeles, Los Angeles, CA 90095, USA

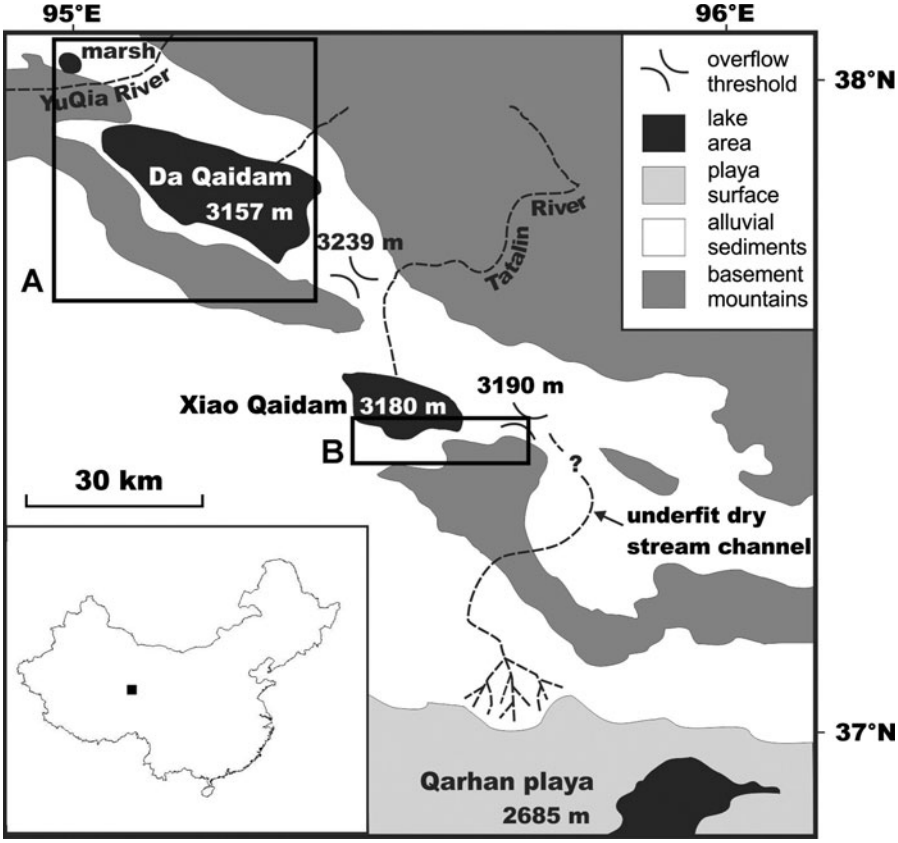

Fig. 1 Map of the Da Qaidam/Xiao Qaidam lakes region in the southeastern Qaidam Basin, China, showing the location of important geomorphic features discussed in the text. Lake and overflow threshold elevations above sea level are approximate. *Inset***a**: area shown in Fig. 2a. *Inset***b**: area shown in Fig. 6

now lie outside the primary influence of both the Indian and East Asian summer monsoons (Tian et al. 2001; Herzschuh 2006; Vandenberghe et al. 2006). Past work at the lakes has suggested they were markedly enlarged during MIS 3 (Huang et al. 1981; Chen and Bowler 1986; Zheng et al. 1989; Yu et al. 2001), and this interpretation of the lakes' histories has contributed substantially to the notion there was a "Greatest Lakes" period across the Tibetan Plateau and northwestern China during the last interstadial period (Li 2000; Zheng et al. 2000; Jia et al. 2001; Li and Zhu 2001; Shi et al. 2001; Yu et al. 2001; Yang et al. 2004; Owen et al. 2006; Wünnemann et al. 2007; Yang and Scuderi 2010).

This interpretation of MIS 3 mega-lakes, however, contrasts sharply with interpretations derived from other climate proxy records suggesting that maximum early MIS 3 effective moisture was similar to or only slightly greater than the Holocene maximum and that the later MIS 3 period was even drier (Fang et al. 1999; Herzschuh 2006; Ning et al. 2009; Jiang et al. 2011; Long et al. 2012a, b). This difference has led to the conclusion that the "…anomalously high" MIS 3 lakes are something of "an enigma" (Colman et al. 2007). A number of recent studies of lake shorelines on the northeastern margin of the Tibetan Plateau suggest that, at some lakes at least, the high stands thought to date (by ^{14}C) to MIS 3 actually date [by optically stimulated luminescence (OSL)] to the MIS 5 interglacial period, and that maximum MIS 3 shorelines were, as suggested by the loess and plant-based climate reconstructions, at or near the elevations of Holocene highstands (Madsen et al. 2008; Fan et al. 2010; Liu et al. 2010; Rhode et al. 2010; Long et al. 2012a; Zhang et al. 2012). Moreover, it is becoming increasingly apparent that tectonic and geomorphic processes are often responsible for shoreline formation in a number of northwestern China lake basins and may be inappropriate for use as paleoclimate proxy records (Chen et al. 2008a; Dietze et al. 2010; Hartmann et al. 2011).

As a result, we engaged in a multi-year project focused on identifying and dating shoreline features at many of these supposed MIS 3 mega-lakes. Here, we report a revised interpretation of the Da Qaidam and Xiao Qaidam lake histories based on the basins' geomorphology, reanalysis of previous work, and new OSL age estimates of the highest shoreline features in the basins.

Setting

The Xiao Qaidam and Da Qaidam lakes lie at the southwestern margin of Dakendaban Mountain, and are centered at UTM 46 s, 721830E, 4152370N and 690960E, 4192380N, respectively. The relatively small lake basins are part of the larger Da Qaidam Basin, a foreland basin of the Qilian Shan belt (Wang et al. 2006). Dakendaban Mountain is part of the Qilian Mountains and the lakes are fed by winter snow melt from this range combined with summer precipitation in the drainages. Xiao Qaidam is fed primarily by the Tatalin River (Fig. 1a), whereas Da Qaidam is fed by four small seasonal streams from short drainages on the western flank of Dakendaban Mountain.

Da Qaidam is now a shallow, saline lake/playa system that varies seasonally in surface area from $\sim$23 to 36 km^2, with the area of the playa reaching $\sim$240 km^2. Depth varies similarly, rising less than 1 m during the summer flood season (Zheng et al. 1989), and we have noted $\sim$1–2 m inter-annual variation over the last decade. The surface elevation of the lake was $\sim$3,155–3,160 m a.s.l. in 2010–2011, varying slightly across the lake's surface due to impoundments for salt evaporation. Xiao ("little") Qaidam, located southeast of Da ("big") Qaidam, is actually the larger of the two lakes at present, with a surface area varying from $\sim$40 to 70 km^2, and is somewhat deeper, varying seasonally between 1–3 m deep. However, its playa surface is smaller, at $\sim$150 km^2 (Yu et al. 2001).

An alluvium-covered threshold with a minimum surface elevation of $\sim$3,239 m a.s.l., separates the two lake basins. The different surface elevations of the lakes suggest there is a bedrock threshold at an unknown depth below the surface alluvium. The playas in the two basins tilt slightly in opposite directions away from this threshold, with Xiao Qaidam tilting to the south from $\sim$3,190 m a.s.l. to the lake surface at $\sim$3,177–3,179 m in 2010–2011. The Da Qaidam playa, on the other hand, is at $\sim$3,185 m near the threshold, and slopes downward to the north. The similarity of the playa elevations adjacent to the threshold suggests that the threshold between them may have been elevated by isostatic rebound or other tectonic processes.

The drainage basins feeding the lakes lie well north and/or west of the present main influence of the Indian and East Asian monsoons (Tian et al. 2001; Herzschuh 2006; Vandenberghe et al. 2006) and the region is very dry and cold. The average annual precipitation at the town of Da Qaidam is 83.5 mm and the average annual temperature is 1.4° C. What precipitation there is comes primarily during the summer months, with infrequent intense storms producing extensive runoff floods in otherwise dry years. Average annual evaporation at Da Qaidam is 2,032 mm.

Previous research

The known Da Qaidam lake history is drawn primarily from numerous drill core assays conducted for mineral extraction in the greater Qaidam Basin. Based on these core records, Zheng et al. (1989) concluded that a large megalake occupied the joint Da/Xiao Qaidam basins before $\sim$30 ka BP. Halite layers above basal lacustrine clays also suggested an episodic dewatering of the basin during MIS 2 and the Holocene. Chronological controls for the sequences are provided by the dating of two short-cores collected and reported by Huang et al. (1981) and reassessed by Yu et al. (2001). Core CK3, taken from a location near the center of the Da Qaidam basin, is 11 m long and contains an undated yellow lacustrine mud at its base. This is overlain by black organic-rich lacustrine mud containing borate and gypsum in low percentages, which suggests the lake was shallowing during this depositional interval. A radiocarbon age estimate of $\sim$21 ^{14}C ka BP ($\sim$25 cal ka BP), run on a bulk organic sample, was obtained from near the base of this unit. Sediments higher in the core consist of units containing varying amounts of evaporate minerals, suggesting episodic freshening of lake waters (Huang et al. 1981; Yu et al. 2001). The ages of these episodes are controlled by two additional ^{14}C dates. The second core, CK2022, was collected by Huang et al. (1981) from Bieletan Lake about 120 km southwest of Da Qaidam in the Qarhan Basin, although Yu et al. (2001) describe this lake as being in a sub-basin of the Da Qaidam lake basin. The black lacustrine muds at the base of this 101-m core were dated at depths between $\sim$96 and 66 m, again using bulk organic samples, to

~32, ~26, ~25, and ~24 ^{14}C ka BP (~37, ~31, ~30, and ~29 cal ka BP). Like core CK3, overlying depositional units in this core consist of alternating, more or less saline sediments with the ages controlled by three additional ^{14}C age estimates.

Although these core records are not correlated with any shoreline features, Yu et al. (2001) used them to create a lake status record. The earliest deposits are interpreted to indicate a presumably "united Da Qaidam/Xiao Qaidam megalake" that was "maximally high." The lake, in at least the Da Qaidam basin [Yu et al. (2001) are not clear on when they think this posited megalake was divided into separate sub-basins], was thought to be "extremely high" from ~25 to ~22.0 ^{14}C ka BP (~30 to ~26 cal ka BP), and "very high" ~22 to ~20 ^{14}C ka BP (~26 to ~23 cal ka BP). The lake was again "high" from ~10 to ~7 ^{14}C ka BP (~11 to ~8 cal ka BP).

In contrast to Da Qaidam, what is known of the lake history in the Xiao Qaidam basin is derived from shoreline deposits around the lake itself. As part of a program to evaluate the dating of carbonate versus organic muds in saline desert lake systems, Bowler et al. (1986) collected samples from "a series of shore-parallel gravel and beach ridges" 13 m above the lake surface on the lake's southern margin at the time. A sample of clastic carbonate sand from the youngest of the high-water facies produced an age estimate of ~35 ^{14}C ka BP (~40 cal ka BP), whereas an ostracod-shell concentrate from those same sands produced a date of ~15 ^{14}C ka BP (~18 cal ka BP). Bowler et al. (1986) suggest the latter date is more reliable and favor an interpretation of 15–14 ^{14}C ka BP (~18–17 cal ka BP) as the age of the +13 m shoreline.

Archaeological materials in these upper shoreline deposits were identified by Huang et al. (1987) as Upper Paleolithic, based primarily on their presumed technology. The archaeological site, however, was not directly dated. Huang et al. (1987) did not report finding any artifacts representing microlithic technology at Xiao Qaidam, which appear in China after ~20 ka, and, assuming a pre-microblade technology, used dates on the CK2022 core from the Qarhan Basin to suggest an age of ~30 ka for the Xiao Qaidam site. Brantingham et al. (2003, 2007) revisited the site and suggested, alternatively, that the artifacts reported by Huang et al. (1987) are technologically consistent with those dating to the early Holocene at other sites on the northern Tibetan Plateau.

Sun et al. (2010) applied OSL dating methods to lacustrine sediments (localities XCDH1 and XCDH3) they thought to be 4–5 m above the site (XCDH2) and determined they were deposited ~11–3 ka. They concluded the site was: "(1) younger than ~3 ka if the lake terrace of XCDH2 is younger than the terrace represented by XCDH1 and XCDH3; or (2) between ~3 and ~11 ka if these two terraces are part of the deposit of the same time period" (Sun et al. 2010: 360). They also identified near-shore lacustrine deposits they thought to be ~40 m above the present lake on its southwestern margin. These were dated to ~51–37 ka. However, they note that the dose rates for the two samples from these lacustrine deposits were much higher than those from the lower shoreline, but attributed that difference to possible differences in sediment sources. No shoreline features have been associated with these higher lacustrine deposits.

Materials and methods

Field methods

We conducted fieldwork in the Da Qaidam and Xiao Qaidam basins for short intervals in 2001 and 2002, and then again in 2009 and 2011. Paleoshorelines and various aspects of the basins' geomorphology were first identified in the field, examined and mapped on satellite imagery, and then rechecked once again upon our return to the lake basins. A limited number of OSL samples were collected in 2009 for preliminary chronological assessments and a single sample was collected in 2011. Samples were collected from existing exposures. These were cleaned back by at least 50 cm, described and photographed. Steel tubes, 22 cm long by 4 cm diameter, were then driven into the cleaned vertical sections. Each tube was covered with black cloth and sealed in a black plastic bag, then wrapped with tape to avoid light exposure and moisture loss. In the laboratory, sediments at each end of the cylinders were scraped away and used for water content and dose rate measurements. The single AMS radiocarbon age determination we obtained was run on a sample of unidentified plant seeds handpicked from a sample collected from an exposed organic lens.

Elevations of these sampling localities, and other critical locations shown in Figs. 2 and 3, were determined using a differential GPS system tied to

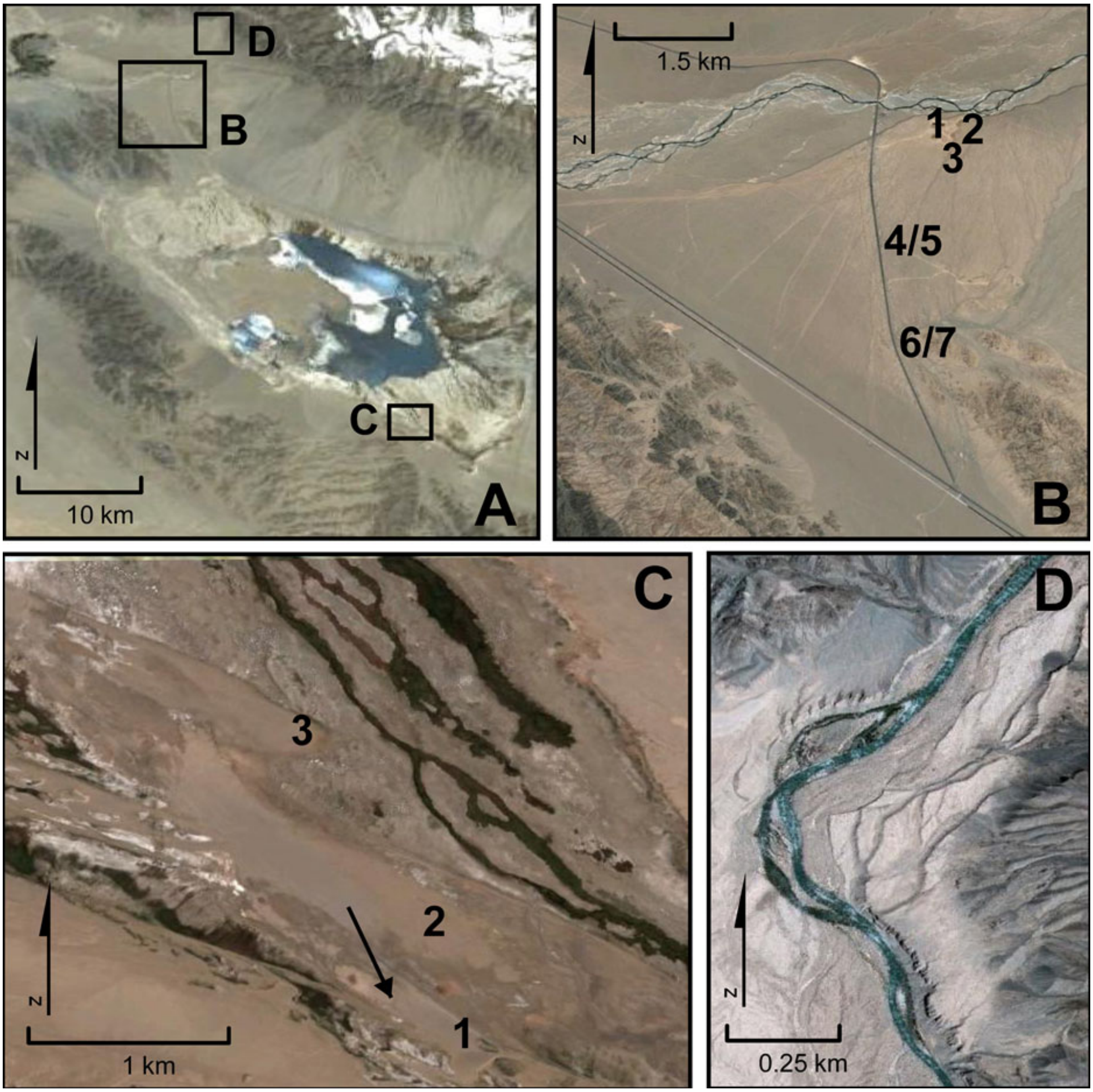

Fig. 2 **a** Satellite image of the Da Qaidam basin and internal features discussed in the text. **b** Paleo alluvial fan formed by the YuQia River (to the north of the paleodelta) when it fed Da Qaidam, and OSL sampling locations YQ-1A (~9.2 ka), YQ-1B (~10.5 ka), YQ-2 (~23.6 ka), YQ-3 (~15.8 ka), YQ-4 (~21.7 ka), YQ-5 (~17.0 ka), YQ-6A (~2.8 ka), YQ-6B (~5.0 ka), and YQ-7 (~15.0 ka). **c** Regressive phase spit sequence on the southeastern margin of Da Qaidam: (*1*) highest shoreline spit (elevation ~3,180 m a.s.l.), (*2*) intermediate spit (~3,172 m), (*3*) lower spit (~3,168 m), *arrow* shows OSL sampling locations DQ-1A (~94.8 ka) and DQ-1B (~113.8 ka). **d** YuQia River terrace sequence at the mouth of Dakendaban Mountain canyon. The highest terrace to the right is also the head of the paleofan

lake elevations in 2011 (~3,180 m a.s.l. for Xiao Qaidam and ~3,157 m for Da Qaidam). Unfortunately, absolute lake level elevations are not officially recorded and there is not a national survey data point sufficiently close to allow extrapolation to the lakes. As a result, although we consider the elevations of the sample localities to be accurate relative to one another, estimated elevations above sea level are derived using a combination of map data and elevations from Google Earth. Although less accurate, based on our experience

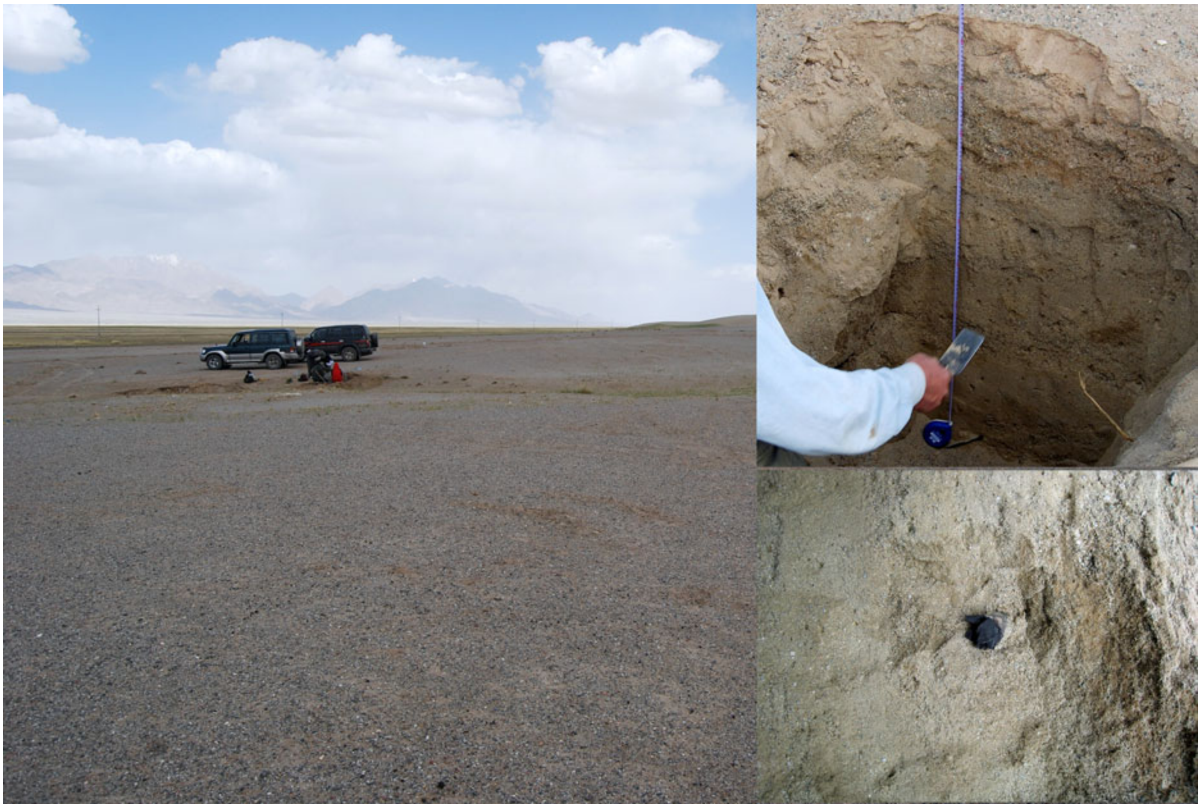

Fig. 3 OSL sampling locality on the surface of a spit at the highest apparent shoreline in the Da Qaidam basin. *Inset* images illustrate the sand and fine gravel nature of the spit sediments in the sampling profile. Sampling tube is 4 cm in diameter

working in other nearby lake basins, these estimated elevations are usually within 2 m of those determined by differential GPS.

Dating methods

We used OSL methods to produce age estimates for 12 samples collected from the Da Qaidam basin and a single sample from the Xiao Qaidam basin (Table 1). Laboratory preparation included treatment with HCl (10 %) and H_2O_2 (30 %) to remove carbonates and organics, respectively, and dry sieving to isolate the 38–63 μm fraction. The fraction was then treated with 35 % H_2SiF_6 for 2 weeks to remove feldspars (Berger et al. 1980; Roberts 2007; Lai 2010). The resulting quartz grains were washed with 10 % HCl and water. Quartz purity was monitored by IR stimulation. Any samples with measurable IRSL signals were retreated with H_2SiF_6 to avoid D_e underestimation (Roberts 2007; Lai and Brückner 2008). Pure quartz grains were then deposited on the center (diameter [dia.] ~3–4 mm) of stainless steel disks (dia. 10 mm) using silicone oil. OSL measurements were carried out on a Risø TL/OSL-DA-20 reader. Stimulation was by blue LEDs (470 ± 20 nm) for 40 s at 130° C, and detection was through 7.5-mm Hoya U-340 filters. The single aliquot regenerative-dose (SAR) protocol (Murray and Wintle 2000) was used for equivalent dose determination (D_e). Preheat was at 260° C for 10 s, determined after plateau and dose recovery tests. Preheat plateau and dose recovery tests (Murray and Wintle 2003) were conducted on samples DQ-1A and YQ-2 to determine the preheat plateau. The preheat plateau test showed that there was a plateau from 220 to 280 °C, and that the lab dose could be recovered within 10 % error. Cut-heat was at 220 °C for 10 s. We use a higher temperature cut-heat to ensure that if any laboratory-dose-induced ultra-fast OSL component existed it was removed by the thermal treatment to avoid potential D_e underestimation (Jain et al. 2003).

Signals from the first 0.64 s of stimulation were integrated for growth curve construction after

Table 1 Sample information, environmental radioactivity and OSL dating results

Sample number	Location (UTM: 46 s)	Sediment type	Depth (m)	Grain size (μm)	K (%)	Th (ppm)	U (ppm)	Aliqu. Num.	Dose rate (Gy/ka)	De (Gy)	OSL age (ka)
DQ-1A	699575E 4180627N	Lacustrine sand	0.30	38–63	1.242 ± 0.045	4.830 ± 0.121	1.165 ± 0.094	35	2.23 ± 0.15	210 ± 7	94 ± 8
DQ-1B	699573E 4180634N	Lacustrine sand	0.90	38–63	1.053 ± 0.041	3.442 ± 0.093	1.632 ± 0.096	36	2.05 ± 0.14	232 ± 8	113 ± 8
YQ-1A	684107E 4209054N	Aeolian sand	0.30	38–63	1.73 ± 0.059	5.485 ± 0.148	1.142 ± 0.116	36	2.76 ± 0.20	25.5 ± 1	9.2 ± 0.7
YQ-1B	684387E 4209111N	Aeolian sand	0.05	38–63	1.639 ± 0.052	4.996 ± 0.125	1.067 ± 0.091	36	2.61 ± 0.19	27.3 ± 0.9	10.5 ± 0.8
YQ-2	684186E 4209054N	Alluvial sandy gravel	0.20	38–63	1.168 ± 0.042	3.686 ± 0.100	1.33 ± 0.090	36	2.12 ± 0.14	50.1 ± 2.7	23.6 ± 2.0
YQ-3	684222E 4209060N	Aeolian sand	0.25	38–63	1.267 ± 0.047	5.955 ± 0.149	2.662 ± 0.136	36	2.79 ± 0.02	44.0 ± 1.9	15.8 ± 1.2
YQ-4	683443E 4207537N	Alluvial sand lens	1.20	38–63	1.741 ± 0.056	10.660 ± 0.231	2.1 ± 0.13	36	3.36 ± 0.23	73.0 ± 1.7	21.7 ± 1.7
YQ-5	683450E 4207527N	Alluvial sand lens	1.25	38–63	1.671 ± 0.057	10.690 ± 0.246	2.231 ± 0.136	36	3.40 ± 0.23	57.7 ± 1.5	17.0 ± 1.2
YQ-6A	683528E 4206315N	Alluvial sand lens	0.20	38–63	1.685 ± 0.059	10.880 ± 0.250	2.450 ± 0.149	36	3.53 ± 0.25	9.9 ± 0.3	2.8 ± 0.2
YQ-6B	683512E 4206318N	Alluvial sand lens	0.60	38–63	1.519 ± 0.053	6.416 ± 0.154	2.517 ± 0.128	36	3.00 ± 0.20	15.1 ± 0.9	5.0 ± 0.5
YQ-7	683614E 4206280N	Alluvial sand lens	0.60	38–63	1.252 ± 0.041	5.193 ± 0.130	3.031 ± 0.139	36	2.80 ± 0.18	41.9 ± 1.0	15.0 ± 1.0
XQ-1	727400E 418820N	Alluvial sand lens	6.80	38–63	2.230 ± 0.029	6.660 ± 0.157	1.340 ± 0.223	36	3.16 ± 0.23	301 ± 18	95 ± 9

background subtraction, using the signal in the shine-down curve of the last 5 s. A quartz OSL growth curve for sample DQ-1b, with a regeneration dose up to 800 Gy, is shown in Fig. 4. Water content was taken as 5 ± 5 % for all samples because the study area is arid, with precipitation less than 100 mm per year. In the OSL community, the water content for loess in the Chinese Loess Plateau (a semi-arid area with precipitation of about 250–400 mm per year) is normally taken as 10 % (Lai and Wintle 2006). We therefore assigned 5 % for the samples from the much drier area of our study.

Concentrations of U, Th and K were obtained by neutron activation analysis. For the 38–63 μm grains, an alpha efficiency (a value) of 0.035 ± 0.003 (Lai et al. 2008) was adopted. The cosmic ray dose rate was estimated for each sample as a function of depth,

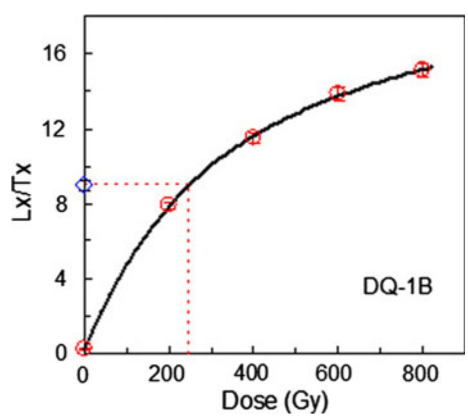

Fig. 4 Quartz OSL growth curve for sample DQ-1B measured by SAR protocol. Signals of the initial 0.64 s stimulation were integrated after background subtraction. Note the growth curve is not saturated with a regeneration dose up to 800 Gy. The *circles* represent the regeneration doses

altitude and geomagnetic latitude (Prescott and Hutton 1994). Finally, elemental concentrations were converted into annual dose rates according to Aitkin (1998).

The mean calendar ages of radiocarbon age estimates discussed here were obtained using Calpal-Online (http://www.calpal-online.de) to provide comparison to the calendrical OSL age estimates. Unless otherwise specified, all ages are given in calendar years and rounded to thousands of years (ka).

Geomorphological and depositional setting of OSL samples

Da Qaidam shorelines

We investigated shoreline features around Da Qaidam in 2001 and 2002. Preliminary OSL samples from the highest identified shoreline were collected in 2009. The eastern and northern margins of the lake are covered by late Pleistocene and Holocene alluvium and no shoreline features are visible. A series of shoreline features consisting primarily of barrier bars and spits, however, is exposed on the lake's southwestern edge (Fig. 2a, c). We collected two OSL samples from a 1.5-m-deep pit excavated into the side of a small erosional channel cutting the crest of the highest spit at an elevation of ~3,176 m a.s.l. (Figs. 2c, 3). Lake-shore sediments at this exposure consist of horizontally (east–west) bedded fine gravels to medium sand. Samples DQ-1A and DQ-1B were collected at depths of 30 and 90 cm below surface.

Da Qaidam/YuQia River alluvial history

The toe of an alluvial fan formed by the YuQia River reaches the northeastern margin of Da Qaidam, and paleochannels on the fan's surface suggest the river once flowed into the lake, at least at times (Fig. 2a, b). The YuQia River is now inset into this older fan and flows into Mahai Lake in the northern Qarhan Basin to the northwest rather than into Da Qaidam. Paleochannels on this abandoned fan suggest that as the river shifted back and forth across the fan it alternatively fed Da Qaidam and a smaller basin immediately to the west (Fig. 1, "marsh"). At some time in the past, the gradient of the YuQia River changed as a consequence of tectonic shifts and/or down-cutting through a bedrock threshold southwest of the smaller basin. At mid-fan elevations, the river's surface waters now are ~10 m below the paleofan surface. We attempted to determine when the YuQia River last flowed into Da Qaidam by collecting a series of limiting OSL samples from deposits overlying the paleochannels and from samples collected from alluvial sediments in or cut by the channels.

Three limiting OSL samples, YQ-1A, YQ-1B, and YQ-3, were collected in aeolian sand deposited against the slumped channel margins of YuQia River paleochannels [Fig. 2b (1, 3)]. Three other samples collected from a secondary channel terrace inset into an older YuQia River paleochannel also provide limiting age estimates [Fig. 2b (6, 7)]. Water in this younger channel presently derives from a small Dakendaban Mountain glacial cirque drainage immediately to the southeast of the YuQia River canyon. Seasonal and intermittent storm-generated stream flow from the cirque drainage has captured a YuQia River paleochannel where the smaller alluvial fan merges with the much larger YuQia fan. Samples YQ-6 A & B were collected from sand lenses within coarse gravel and cobbles (to 15 cm dia.) at depths of 20 and 60 cm below surface of the inset secondary terrace. Sample YQ-7 was collected from a sand stringer on the opposite margin of the secondary channel at a depth of 60 cm below surface.

Three OSL samples directly dating channel formation were collected from the fluvial/alluvial fill of paleochannels flowing into the Da Qaidam basin. Sample YQ-2 was collected from a shallow pit excavated into fluvial/alluvial sediments underlying an accretionary soil developed on a fan surface channel interfluve (Figs. 2b[2], 5). Sediments underlying the accretionary soil consist of heavily carbonate-coated cobbles and coarse gravels mixed with some sand. A very well developed soil in these deposits has broken down much of the material into clay. Samples YQ-4 and YQ-5 were collected from fluvial/alluvial sediments exposed in a small gravel quarry excavated within a paleochannel [Fig. 2b (4, 5)]. The surface of the alluvial fan at this location has been disturbed by the quarrying operations and the relationship of the sediments to the paleochannel is unclear. Sample YQ-4 was collected from a sand lens 1.2 m below the top of the disturbed surface. YQ-5 was collected from a second sand lens 1.25 m below the disturbed surface in an exposure 25 m to the southwest. Gravels in the fluvial/alluvial sediments are carbonate cemented, but individual cobbles have only a slight carbonate coating. A ~10-cm-thick accretionary soil is developed on the alluvial fan surface outside the quarry area and a relatively well developed soil on the alluvial sediments themselves. The alluvial sediments are poorly sorted, with individual clasts reaching 50 cm diameter. The sediments are characterized by thick gravel lenses, with coarse sand stringers.

Xiao Qaidam

Results from study of geomorphological features in the Da Qaidam basin led us to re-evaluate selected geomorphic features in the Xiao Qaidam basin as well. Although we could collect only a single new age estimate for Xiao Qaidam shoreline features, the nature of these geomorphic features suggests a re-interpretation of previously acquired age estimates is required. Most importantly, we determined that the present threshold control for the Xiao Qaidam basin is located southeast of the lake at the crest of a *bajada* that separates the basin from a drainage leading into the Qarhan Basin to the southwest [Fig. 6 (6)]. This alluvium-covered overflow threshold is centered 7–9 km east of the lake's present southeastern margin (UTM 46 s, 736100–737760E, 4148600N).

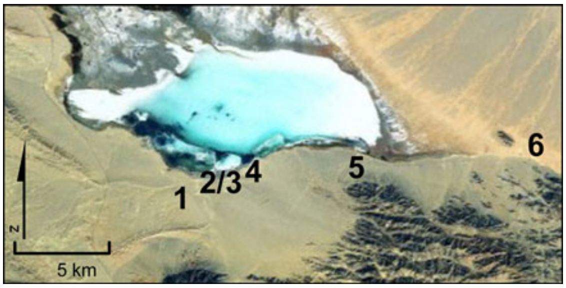

Fig. 6 Satellite image of the southern Xiao Qaidam lake margin showing OSL sampling locations and the alluvium-covered overflow threshold: (*1*) location of isolated lacustrine deposits at ~30 m above the modern lake (XCDH4); (*2*) locality XCDH1; (*3*) locality XCDH3; (*4*) Xiao Qaidam archaeological site (XCDH2); (*5*) gravel quarry sample location; (*6*) overflow threshold ~10–12 m above the lake surface

In 2011 we measured the elevation of the threshold surface to be 10–12 m above the lake (~3,190–3,192 m a.s.l.). The elevation of any possible bedrock sill below this surface Holocene alluvium, although unknown at present, is likely at least several meters lower. This low threshold elevation suggests that Xiao Qaidam may have overflowed into the Qarhan Basin in the past. At present,

Fig. 5 OSL sampling location YQ-2 (*arrow*) at the proximal end of one of the most recent YuQia River channels on the paleofan surface that terminates in the Da Qaidam basin. The profile exposing a cross-section of the channel fill (*dotted line*) is the result of the incision of the modern YuQia River into the older paleofan sometime after ~23–17 ka

water seeping through the fan emerges ~20 km ESE of Xiao Qaidam at the fan's eastern margin. This water forms a small intermittent stream that follows an older channel south into the Qarhan Basin (Fig. 1). This small stream is underfit for this older channel, indicating stream flow was much greater in the past. This paleochannel has roughly the same morphology as that of the Tatalin River that presently feeds Xiao Qaidam (Fig. 1), suggesting it may have been Tatalin River waters that originally fed the paleochannel.

We also measured the elevation of the higher lacustrine deposits at locality XCDH4 [Fig. 6 (1)], dated by Sun et al. (2010) to ~51–37 ka, and found them to be at ~3,210 m, ~30 m above the modern lake surface, rather than ~40 m as previously reported. However, that is still >15 m above the alluvium-covered threshold elevation. This suggests there has been considerable tectonically driven change in the shape of the basin since these lacustrine sediments were laid down. These lake deposits are found only along the southwestern margin of the lake where a bedrock outcrop near the shoreline has protected them from erosion by the late Quaternary alluvial cut-fill sequences surrounding most of the basin. The exposed sediments represent offshore deposition and no shoreline features are evident.

To provide a preliminary test of the age estimates of Sun et al. (2010), we obtained a single OSL sample (XQ-1) from a gravel quarry excavated into late Quaternary alluvium east of the XCDH4 locality, where the upper lacustrine deposits were not protected from erosion by a bedrock outcrop [Fig. 6 (5)]; UTM 46 s, 727390E, 4148800N). The surface of the alluvial *bajada* in this area extends from an elevation of ~3,350 m a.s.l. in the south to ~3,184 m (~4–5 m above the lake surface in 2011) in the north and the alluvium necessarily post-dates the high lacustrine deposits. The gravel quarry is located toward the toe of this *bajada* and has a surface elevation of 23–26 m above the 2011 lake surface (~3,203–3,206 m a.s.l.), and 4–7 m below the deep-water lacustrine deposits at locality XCDH4. There are 9 m of alluvium exposed in the quarry (Fig. 7). The upper 2.5–3.0 m consist of poorly cemented coarse gravel to small cobbles with some sand lenses. This is underlain by 3 m of well-cemented gravels containing a well-developed soil. The lower section of the exposed sediments consists of poorly cemented laminated sands and gravels. We collected OSL sample XQ-1 from the center of one of these 22-cm-thick sand lenses 6.8 m below the surface, or ~19 m above the modern lake in 2011, ~7–9 m above the Xiao Qaidam threshold surface, and ~10–11 m below the elevation of the lacustrine deposits at locality XCDH4.

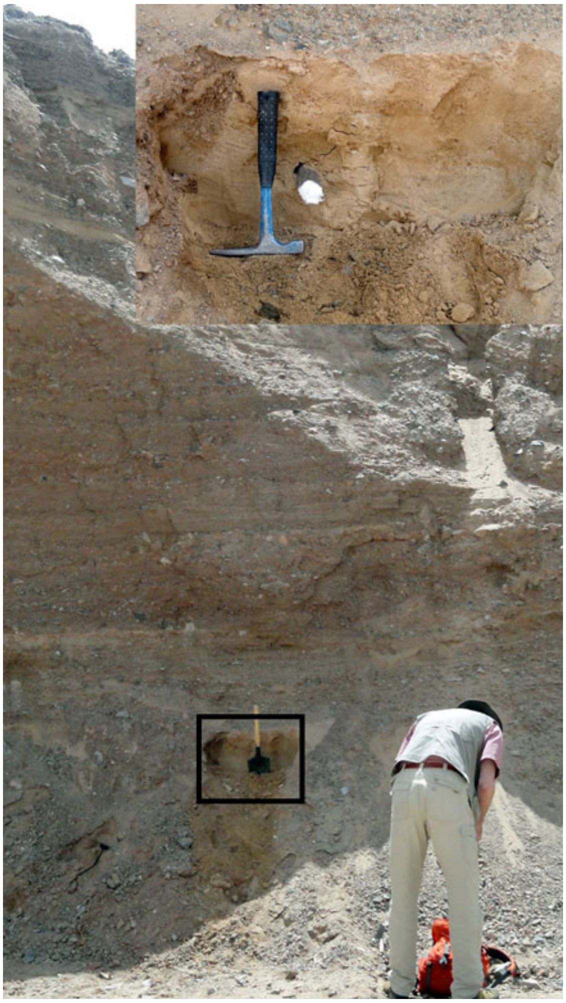

Fig. 7 View of alluvial fan sediments in gravel pit exposure (No. 5 in Fig. 6) at OSL sampling location XQ-1 (~95.0 ka). *Box* indicates the location of the inset image showing the OSL sampling tube within the 22-cm-thick sand lens at a depth of 6.8 m in the alluvial sequence

Xiao Qaidam archaeological site

We also reexamined the localities thought by Sun et al. (2010) to provide age estimates for the archaeological site on the southern margin of Xiao Qaidam reported by Huang et al. (1987). Sun et al. (2010) did not date the archaeological site directly, but rather obtained a series of OSL samples from two localities, XCDH1 and XCDH3, west of the lake terrace on which the archaeological site rests [Fig. 6 (2, 3)]. They estimated the two localities to be above the elevation of the archaeological site and therefore considered that the age estimates from those localities were useful in limiting the age of the site to between 11 and 3 ka. In 2011, however, our measured elevations of the two adjacent localities indicate their surfaces were only 2 m above the lake surface, whereas that of the sloping alluvium-covered terrace on which the archaeological site rests (XCDH2) was 4-7 m above the modern lake [Fig. 6 (4)]. As a result, the OSL age estimates obtained from the two localities by Sun et al. (2010), ranging from ~11 to 3 ka, do not appear to be useful in limiting the age of the archaeological site. With a single exception, the sediments exposed at the two localities are composed of shoreline sands and gravel, suggesting that the lake fluctuated near this elevation throughout most of the Holocene. At locality XCDH1, however, a thin lens of ripple-laminated, fine-grained, near-shore sand occurs 20–25 cm below the modern sediment surface and above an OSL age estimate of ~3 ka obtained by Sun et al. (2010). This suggests a late Holocene transgression to an elevation of ~3 m above the 2011 lake surface elevation.

In addition, we conducted a surface reconnaissance of the site, first identified by Huang et al. (1987) and revisited by Brantingham et al. (2007), and collected a small (n = 25), unsystematic assemblage of stone tools from the surface. The raw materials appear to be typical for this portion of the Tibetan Plateau. Most of the specimens (n = 18) are fine-grained quartzite that varies in color from brown to gray-brown and green. Four specimens are made of intermediate-quality red jasper. Two specimens are a coarse-grained, white-tan quartzite, consistent with previous finds at the site (Huang et al. 1987; Brantingham and Gao 2006). There are two technologies, represented by five specimens, which would be traditionally considered to be chrono-stratigraphically diagnostic. The remaining specimens (n = 20) are generic flakes that are technologically non-diagnostic.

Microblade technologies are unambiguously present, in the form of two formally shaped, pebble-based microblade cores, as well as numerous microblades and microblade fragments that were not collected from the site. These are considered to be <15 ka in age and probably <11 ka in age based on other sites on the Tibetan Plateau (Brantingham et al. 2007). The other seemingly diagnostic technology consists of three artifacts with technical elements consistent with Upper Paleolithic Levallois-like, broad-faced cores. All three specimens in question would not be out of the ordinary in Shuidonggou #1, a diagnostically important Upper Paleolithic site in Ningxia Province in northwest China, dating to ~33–27 ka (Gao et al. 2002; Guan et al. 2011). They would also fit (except for raw material) very neatly with the Paleolithic tool collection from Chickhen Agui, a rock shelter site in the Mongolian Gobi dating to ~31 ka (Derevianko et al. 2004).

Results and discussion

Da Qaidam shoreline chronology

The highest Da Qaidam shoreline feature we could locate is at an altitude of ~3,180 m a.s.l. (~23 m above the lake surface in 2011) and we could detect no wave-cut platforms or depositional features on the mountain front immediately west of this shoreline. Alluvium, however, covers elevations between ~3,180 and 3,195 m a.s.l. Additional spits and bars are found at elevations of ~8–12 m below the highest shoreline features, but have similar weathering characteristics and appear to represent a series of recessional still-stands as the lake regressed from its highest elevation. The spits all trend to the south, as does the foreset bedding exposed in several small excavations, indicating long-shore lake currents flowed primarily in a counter-clockwise fashion around the lake. The sediments in these shoreline features are relatively fine-grained, consisting of sand and small gravel. There are, however, few large exposures available for examination. The gravels are sub-angular to sub-rounded, averaging ~0.3–0.5 cm diameter, rarely reaching 2.0 cm diameter. A relatively well-developed soil is formed in the upper 25 cm of the deposits and the upper 5 cm is lightly cemented by calcium carbonate.

The age estimates for the two samples from the highest observed shoreline, DQ-1A and DQ-1B, are 94 ± 8 and 113 ± 8 ka, respectively (Table 1). The two ages are similar within 2 sigma error. We therefore conclude the shoreline deposits at this location were laid down ~100 ka, during MIS 5.

Da Qaidam/YuQia River alluvial chronology

The age estimates for limiting samples YQ-1A, YQ-1B, and YQ-3, collected from aeolian sand deposited against paleochannel margins of the YuQia River alluvial fan, are 9.2 ± 0.7, 10.5 ± 0.8, and 15.8 ± 1.2 ka, respectively (Table 1). Limiting age samples YQ-6A, YQ-6B, and YQ-7, collected from the inset Dakendaban Mountain channel, produced age estimates of 2.8 ± 0.2, 5.0 ± 0.5, and 15.0 ± 1.0 ka, respectively. Samples YQ-2, YQ-4, and YQ-5, collected from paleochannel deposits on the surface of the YuQia River paleofan, provide direct age estimates of 23.6 ± 2.0, 21.7 ± 1.7, and 17.0 ± 1.2 ka, respectively, with a weighted average of 19.4 ± 0.9 ka.

Based on these direct age estimates on samples from alluvial fan sediments in the paleochannels that flowed into Da Qaidam, and on limiting age estimates from sediments overlying the paleochannels, we conclude that YuQia River waters last fed Da Qaidam sometime between ~23 and 17 ka. What caused the gradient of the YuQia River to shift is unclear. A series of river terraces at the canyon mouth where the river exits Dakendaban Mountain suggests the river down-cut through its older alluvial fan in an episodic fashion. At least six terraces, including the highest paleofan surface, are evident at the canyon mouth (Fig. 2a, d). These terraces suggest periods of rapid down-cutting followed by stabilization of the river's base level.

There may also have been some down-cutting through the YuQia River canyon, northwest of Da Qaidam. The small basin at the toe of the southwestern margin of the YuQia River paleofan was also apparently fed, and possibly formed, by the river when it shifted away from Da Qaidam drainages. The basin has now been dewatered and we were able to collect a sample of unidentified seeds (cf. Juncaceae) from marsh deposits at a depth of 1.53–1.58 m below the present surface in the basin. The sample produced a ^{14}C age estimate of 4,290 ± 40 ^{14}C BP (~4.9 cal ka BP), suggesting this dewatering event took place sometime between 16 and 5 ka BP.

Xiao Qaidam chronology

We determined the altitude of the highest lacustrine deposits dated by Sun et al. (2010) to be well below the surface of the ~3,239 m threshold separating the Da Qaidam and Xiao Qaidam basins. Their relationship to a possible bedrock threshold between the two basins is unknown. As noted previously, we could detect no shorelines above ~3,180 m a.s.l. in the Da Qaidam basin that would provide evidence of a megalake joining the two basins. We conclude that no such megalake existed in at least the last ~100 ka (the preliminary age estimate of the much lower elevation lake features in the Da Qaidam basin), and that these higher lacustrine deposits in the Xiao Qaidam basin must therefore represent either a separate late Pleistocene high lake event in the Xiao Qaidam basin or a much older lake that pre-dates the formation of the two lake basins. Because the modern Xiao Qaidam basin threshold surface elevation is >15 m below these lake deposits, we favor the latter interpretation. That, however, brings into question the MIS 3 age estimates reported by Sun et al. (2010).

We reexamined the two samples from locality XCDH4, dated to 37 ± 4 and 51 ± 4 ka. As we noted, Sun et al. (2010) suggested that the high dose-rates of the two samples indicate there may have been different sediment sources for these lake deposits compared to the lower, Holocene-age, deposits. We now think, however, that these age estimates may represent limiting dates and that the ages of the samples are underestimated. When dating loess from the Luochuan section in the Chinese Loess Plateau, Lai (2010) found that for the samples with a D_e <230 Gy (younger than 70 ka), the OSL ages are, within error, in agreement with independent ages established by comparison with marine oxygen isotope stages (Lu et al. 1999). For samples with a D_e >230 Gy, however, OSL ages are severely underestimated, even though the growth curve is still not saturated. For example, a sample collected from below the Brunhes/Matuyama boundary (with an expected age of about 780 ka), the OSL age is only about 107 ka with a D_e of 410 Gy. The mechanism for this underestimation is still unknown (Lai 2010). The two samples from section XCDH4 collected by Sun et al. (2010) both have D_es beyond 230 Gy (246 and 315 Gy, respectively), and their ages are very likely underestimated if the OSL signal characteristics of the quartz are similar to that of the loess reported by Lai (2010).

The age estimate of OSL sample XQ-1 collected from a sand lens within a 9-m-thick alluvial sequence, 10–12 m below the apparently much older deep-water lacustrine deposits, produced an age estimate of ~95 ± 9 ka. The D_e (301 Gy) of this sample is also greater than 230 Gy and it too is likely underestimated. It does, however, suggest the isolated lacustrine sediments on the southwestern margin of the lake may be older than 95 ka.

Age of the Xiao Qaidam archaeological site

Our elevational measurements indicated there are no limiting age controls for the site as suggested by Sun et al. (2010). The mix of Levallois-style and microlithic technologies at the Xiao Qaidam archaeological site suggests two temporal possibilities: (1) the surface materials at the Xiao Qaidam archaeological site represent two chronologically separate occupations of the same locality dating to before and after the Last Glacial Maximum (LGM), or (2) there was a persistence of Levallois-like, broad-faced core production until at least the Pleistocene/Holocene transition. Our recent work at archaeological sites on the northern Tibetan Plateau strongly suggests the latter possibility, but we cannot reject the hypothesis that there was a pre-LGM occupation at Xiao Qaidam until there are better chronological controls for the site.

Lake histories

The late Quaternary lake histories of the Da Qaidam and Xiao Qaidam basins appear to reflect a complex amalgam of climate-induced changes, tectonic events, and geomorphological shifts in river flow. Disentangling this complex history is not a simple task, but direct shoreline age estimates, precise elevational determinations and evaluation of the basin geomorphology are beginning to clarify these lake sequences. These data paint a markedly different picture from those in the past drawn largely from correlations with, and inferences from, other lake basins.

Sedimentary evidence from the oldest, but as yet undated, lake in the two lake basins consists of buried off-shore lacustrine deposits at ~30 m above the modern lake level of Xiao Qaidam (Fig. 8). The presence of an overflow threshold >15 m below these lacustrine deposits, indicates the basin morphology must have been considerably different in the distant past. Considering that the OSL ages of ~51–37 ka obtained by Sun et al. (2010) are considerably underestimated and that we obtained an OSL age estimate of ~95 ka on alluvium below (but chronostratigraphically above) these lacustrine deposits, we tentatively conclude this lake probably dates to well before 100 ka. Huang et al. (1993) suggest that tectonic deformation during the later mid-Pleistocene "…fragmented the earlier large [*Qaidam*] lake basin into a number of secondary or subsidiary basins… [*and*] … the present distribution of lakes essentially reflects the influence of this period." We hypothesize higher lacustrine deposits southwest of Xiao Qaidam may date to before this later mid-Pleistocene period of rapid, tectonically driven change in basin morphology.

After the Da Qaidam and Xiao Qaidam basins achieved their essentially modern form, we see no evidence that the two lakes ever conjoined to form a larger megalake during the late Quaternary. In the Da Qaidam basin we could detect no shoreline features higher than the spits and bars at ~3,180–3,165 m a.s.l. dating to ~100 ka or earlier. Any shoreline features between ~3,165 m and the modern lake surface at ~3,155 m are difficult to discern and are as yet undated. As we noted, fresh-water lacustrine muds dating to older than ~25 ka are evident in drill records (Zheng et al. 1989), but whether these date to MIS 3, 4, 5, or even earlier, is unknown. Why dates on lacustrine muds at the base of a 101-m core from Bieletan Lake in the Qarhan Basin were ever used to infer the age of an MIS 3 lake in Da Qaidam (Yu et al. 2001) or an archaeological site in Xiao Qaidam (Huang et al. 1987) is unclear.

The relationship between possible MIS 3 and Holocene highstands is also complicated by the incision of the YuQia River into its older alluvial fan. Prior to ~23–17 ka, the river flowed into the Da Qaidam basin, at least at times. Thereafter its water no longer fed the Da Qaidam Lake. As a result, climatic inferences comparing MIS 3 and Holocene precipitation regimes based on the Da Qaidam lake history are questionable. Similarly, Tatalin River flow into the lake basins may also have been variable (Fig. 1). The Tatalin River, like the YuQia River, is currently deeply inset into the paleofan at the mouth of the canyon where it exits Dakendaban Mountain. Zheng et al. (1989) suggest the river may have flowed into Da Qaidam during the late Pleistocene and that during the Holocene "east-directed stress produced by the …Altun sinistral fault" caused eastern Da Qaidam to "arch up," forcing the river to shift to the south and flow into Xiao Qaidam. Whereas our own observations support the notion that the divide threshold between the

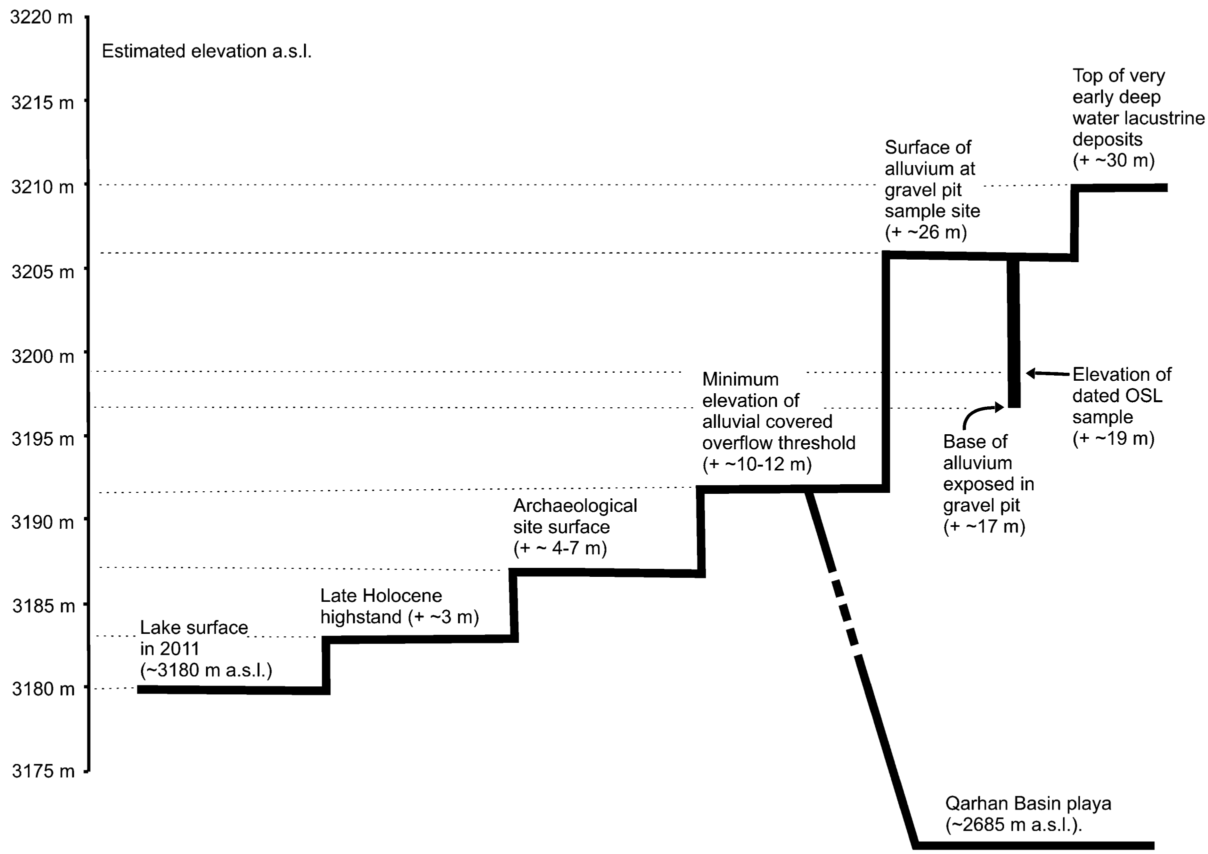

Fig. 8 Schematic diagram illustrating the elevational relationships of features and sampling localities on the southern margin of the Xiao Qaidam basin. Elevations above the lake surface in 2011 were determined using a differential GPS system and we consider them to be accurate relative to one another. Elevations above sea level are estimated, but we consider them to be accurate to within ~2 m

Xiao and Da Qaidam basins has been slightly elevated during the late Pleistocene, it seems more likely that the Tatalin River may have simply shifted back and forth across its fan, as did the YuQia River, flowing alternately into the two basins. Unlike the YuQia fan, there are no evident paleochannels of the Tatalin River terminating in the Da Qaidam Basin, but the shape of the fan itself, with its southwestern margin terminating at Xiao Qaidam and its northwestern margin terminating at the Da Qaidam playa, suggests this likely occurred at times in the past. Furthermore, given that both the YuQia and Tatalin rivers once shifted back and forth across their alluvial fans, alternately feeding one lake basin and then another, use of the lake histories as climate proxies seems problematic.

The lake record in the Xiao Qaidam basin is further complicated by the low elevation of the overflow threshold southeast of the lake. The surface of the alluvial-covered threshold is less than 10 m above the elevation of the lake high stands dated to the late Holocene by Sun et al. (2010) using OSL methods and to ~18 ka by Bowler et al. (1986) using ^{14}C dated ostracod shells. Because a bedrock threshold is likely several meters below this alluvial surface, it appears possible this shoreline is threshold-controlled rather than climatically controlled. Barring any as yet undetected latest Quaternary tectonic shift in the elevation of this threshold, any MIS 3 high stand would also likely not have exceeded this elevation. A late Holocene highstand post-dating ~3 ka may have reached ~3 m above the 2011 lake surface, but apparently did not exceed the elevation of an archaeological site at 4–7 m above the lake and therefore did not approach the threshold.

Conclusions

For a variety of reasons it appears that the late Quaternary lake histories of the Da Qaidam and Xiao Qaidam lakes are not useful climate proxy records and any use of these lake histories to support the notion of a "Greatest Lakes" period in northwest China during MIS 3 is misplaced. Our OSL age estimates are limited and preliminary, but suggest the highest shoreline in Da Qaidam dates to MIS 5 or earlier. Whether even that shoreline relates to climatically rather than geomorphically induced changes is unclear. Based on similarly limited chronological controls, the highest evident lake deposits in the Xiao Qaidam basin appear to be much older than $\sim$100 ka, when the basin's shape was considerably different. The relative precipitation regimes of MIS 3 and the Holocene represented by the Da Qaidam and Xiao Qaidam lake histories are unclear because of the incision of the YuQia River into its fan and its permanent diversion to Mahai Lake in the Qarhan Basin. Comparison of the MIS 3 and Holocene climate regimes represented by the Xiao Qaidam lake history is also difficult, because the elevation of the modern alluvium-covered threshold is only a few meters above the Holocene highstand.

This new Da/Xiao Qaidam lake history record is just one of an increasing number of such revisions produced recently that, together, suggest the notion of an MIS 3 "Greatest Lakes" period in northwestern China must be reassessed. Some of these lakes, thought previously to have records of climatically induced MIS 3 highstands, such as the Jilantai/Hetao megalake in the great bend of the Yellow River, have been, like Xiao Qaidam, proven to be threshold controlled with shoreline histories that are not useful climate proxy records (Chen et al. 2008a). Similar tectonic and geomorphic issues may also complicate the climatic interpretation of lakes in the Gaxun Nur basin, north of the Badain Jaran Desert (Hartmann et al. 2011). Still other lake records, such as those from Qinghai Lake on the northeastern Tibetan Plateau (Madsen et al. 2008; Liu et al. 2010), Gahai Lake in the Qaidam Basin (Fan et al. 2010), Huangqihai Lake in Inner Mongolia (Zhang et al. 2012) and the Zhuyeze paleolake on the western margin of the Tengger Desert (Long et al. 2012a), indicate highest shorelines formed during MIS 5 and that MIS 3 lake levels were only marginally higher than their Holocene highstands.

As yet, however, it may be premature to entirely discount suggestions of high MIS 3 lake levels as being merely a product of curve-matching and extrapolation of lake histories to one another. Yang and Scuderi (2010) and Yang et al. (2011), for example, continue to rely heavily on suggestions of extremely high lake levels during the latter part of MIS 3 to support a climate model incorporating an increase in the intensity of hemispheric Westerlies and a change in summer monsoon penetration. Jiang et al. (2011) note, on the other hand, that most paleoclimate records from east Asia suggest a shift to colder and dryer conditions during the later stages of MIS 3. It remains possible that asynchronous lake histories in western China are a product of differential proximity to the Indian and East Asian monsoons and the prevailing Westerlies (Chen et al. 2008b; Han et al. 2010). Resolution of this issue must await the accumulation of well-documented shoreline histories from across northwestern China and the Tibetan Plateau.

Acknowledgments This work was supported by P.R.C. 973 project (2010CB950202), U.S. National Science Foundation grants 0214870 and 084145, and a Chinese Academy of Science One-Hundred Talent Project (A0961) granted to ZPL. We thank Zhang Biao, E Chongyi, Steffen Mischke, David Page, Evelyn Seelinger, and two anonymous reviewers for assistance with this project.

References

Aitken MJ (1998) An Introduction to optical dating: the dating of Quaternary sediments by the use of photon-stimulated luminescence. Oxford University Press, Oxford, p 267

An ZS, Kutzbach JE, Prell WL, Porter SC (2001) Evolution of Asian monsoons and phased uplift of the Himalaya-Tibetan plateau since Late Miocene times. Nature 411:62–66

Berger GW, Mulhern PJ, Huntley DJ (1980) Isolation of silt-sized quartz from sediments. Ancient TL 11:8–9

Bowler JM, Huang Q, Chen K, Head MJ, Yuan B (1986) Radiocarbon dating of playa-lake hydrologic changes: examples from northwestern China and central Australia. Palaeogeogr Palaeoclimatol Palaeoecol 54:241–260

Brantingham PJ, Gao X (2006) Peopling of the northern Tibetan Plateau. World Arch 38:387–414

Brantingham PJ, Ma HZ, Olsen JW, Gao X, Madsen DB, Rhode DE (2003) Speculation on the timing and nature of Late Pleistocene hunter–gatherer colonization of the Tibetan Plateau. Chin Sci Bull 48:1510–1516

Brantingham PJ, Gao X, Olsen JW, Ma H, Rhode D, Zhang H, Madsen DB (2007) A short chronology for the peopling of the Tibetan Plateau. In: Madsen DB, Chen FH, Gao X (eds)

Human adaptation to climate change in Arid China. Elsevier, Amsterdam, pp 129–150
Chen K, Bowler JM (1986) Late Pleistocene evolution of salt lakes in the Qaidam Basin, Qinghai Province, China. Palaeogeogr Palaeoclimatol Palaeoecol 54:87–104
Chen FH, Fan Y, Chun X, Madsen DB, Oviatt CG, Zhai H, Yang LP, Sun Y (2008a) Preliminary research on megalake Jilantai-Hetao in the arid areas of China during the Late Quaternary. Chin Sci Bull 53:1725–1739
Chen FH, Yu ZC, Yang ML, Ito E, Wang SM, Madsen DB, Huang XZ, Zhao Y, Sato T, Birks HJB, Boomer I, Chen JH, An CB, Wünnemann B (2008b) Holocene moisture evolution in arid central Asia and its out-of-phase relationship with Asian monsoon history. Quat Sci Rev 27:351–364
Colman SM, Yu SY, An Z, Shen J, Henderson ACG (2007) Late Cenozoic climate changes in China's western interior: a review of research on Lake Qinghai and comparison with other records. Quat Sci Rev 26:2281–2300
Derevianko A, Brantingham PJ, Olsen JW, Tseveendorj D (2004) Initial upper paleolithic blade industries from the north-central Gobi Desert, Mongolia. In: Brantingham PJ, Kuhn KL, Kerry KW (eds) The early upper paleolithic beyond Western Europe. University of California Press, Berkeley, pp 207–222
Dietze E, Wünnemann B, Diekmann B, Aichner B, Hartmann K, Herzschuh U, IJmker J, Jin H, Kopsch C, Lehmkuhl F, Li S, Mischke S, Niessen F, Opitz S, Stauch G, Yang S (2010) Basin morphology and seismic stratigraphy of Lake Donggi Cona, north-eastern Tibetan Plateau, China. Quat Int 218:131–142
Fan QS, Lai ZP, Long H, Sun YJ, Liu XJ (2010) OSL chronology for lacustrine sediments recording high stands of Gahai Lake in Qaidam Basin, northeastern Qinghai–Tibetan Plateau. Quat Geochron 5:223–227
Fang X, Ono Y, Fukusawa H, Pan B, Li J, Guan D, Oi K, Tsukamoto S, Torii M, Mishima T (1999) Asian summer monsoon instability during the past 60,000 years: magnetic susceptibility and pedogenic evidence from the western Chinese Loess Plateau. Earth Planet Sci Let 168:219–232
Gao X, Li J, Madsen DB, Brantingham PJ, Elston RG, Bettinger RL (2002) New ^{14}C dates for Shuidonggou and related discussions. Acta Anthropol Sin 21:211–218 (in Chinese)
Guan Y, Gao X, Wang HM, Chen FY, Pei SW, Zhang XL, Zhou ZY (2011) Spatial analysis of intra-site use at a Late Paleolithic site at Shuidonggou, northwest China. Chin Sci Bull 56:3457–3463
Han W, Fang X, Yang S, King J (2010) Differences between East Asian and Indian monsoon climate records during MIS3 attributed to differences in their driving mechanisms: evidence from the loess record of the Sichuan basin, southwestern China and other continental and marine climate records. Quat Int 218:94–103
Hartmann K, Wünnemann B, Hölz S, Kraetschell A, Zhang H (2011) Neotectonic constraints on the Gaxun Nur inland basin in north–central China, derived from remote sensing, geomorphology and geophysical analyses. In: Gloaguen R, Ratschbacher L (eds) Growth and collapse of the Tibetan Plateau. Geological Society, London, Special Pub 353, pp 221–233
Herzschuh U (2006) Palaeo-moisture evolution in monsoonal Central Asia during the last 50,000 years. Quat Sci Rev 25:163–178
Huang Q, Cai BQ, Yu JQ (1981) The ^{14}C age and cycle of sedimentation of some saline lakes on the Qinghai-Xizang Plateau. Chin Sci Bull 26:66–70
Huang WW, Chen KZ, Yuan BY (1987) Paleolithics of Xiao Qaidam Lake in Qinghai Province in China. In: Proceedings of the Sino-Australian Quaternary meeting. Sciences Press, Beijing, pp 168–172 (in Chinese)
Huang Q, Ku T-L, Phillips FM (1993) Evolutionary characteristics of lakes and palaeoclimatic undulations in the Qaidam Basin, China. Chin J Oceanol Limnol 11:34–45
Jain M, Murray AS, Bøtter-Jensen L (2003) Characterization of blue-light stimulated luminescence components in different quartz samples: implications for dose measurement. Rad Meas 37:441–449
Jia Y, Shi Y, Wang S, Jiang H, Li S, Wang A, Li X (2001) Lake-expanding events in the Tibetan Plateau since 40 ka BP. Sci China, Ser D Earth Sci 44(Supplement 1):301–315
Jiang H, Mao X, Xu H, Thompson J, Wang P, Ma X (2011) Last glacial pollen record from Lanzhou (northwestern China) and possible forcing mechanisms for the MIS 3 climate change in Middle to East Asia. Quat Sci Rev 30:769–781
Lai ZP (2010) Chronology and the upper dating limit for loess samples from Luochuan section in Chinese Loess Plateau using quartz OSL SAR protocol. J Asian Earth Sci 37:176–185
Lai ZP, Brückner H (2008) Effects of feldspar contamination on equivalent dose and the shape of growth curve for OSL of silt-sized quartz extracted from Chinese loess. Geochronometria 30:49–53
Lai ZP, Wintle AG (2006) Locating the boundary between the Pleistocene and the Holocene in Chinese loess using luminescence. Holocene 16:893–899
Lai ZP, Zöller L, Fuchs M, Brückner H (2008) Alpha efficiency determination for OSL of quartz extracted from Chinese loess. Rad Meas 43:767–770
Li BY (2000) The last greatest lakes on the Xizang (Tibetan) Plateau. Acta Geograph Sin 35:174–182 (in Chinese with English abstract)
Li BY, Zhu LP (2001) "Greatest lake period" and its palaeoenvironment on the Tibetan Plateau. J Geograph Sci 11:34–42
Liu XJ, Lai ZP, Fan QS, Long H, Sun YJ (2010) Timing for high lake levels of Qinghai Lake in the Qinghai-Tibetan Plateau since the Last Interglaciation based on quartz OSL dating. Quat Geochron 5:218–222
Long H, Lai ZP, Fuchs M, Zhang JR, Li Y (2012a) Timing of Late Quaternary palaeolake evolution in Tengger Desert of northern China and its possible forcing mechanisms. Glob Planet Change 92–93:110–129
Long H, Lai ZP, Fuchs M, Zhang JR, Yang L (2012b) Palaeodunes intercalcated in loess strata from the western Chinese Loess Plateau: timing and palaeoclimatic implications. Quat Int 263:37–45
Lu HY, Liu XD, Zhang FQ, An ZS, Dodson J (1999) Astronomical calibration of loess/paleosol deposits at Luochuan, central Chinese Loess Plateau. Palaeogeogr Palaeoclimatol Palaeoecol 154:237–246
Madsen DB, Ma H, Rhode D, Brantingham PJ, Forman SL (2008) Age constraints on the late Quaternary evolution of Qinghai Lake, Tibetan Plateau. Quat Res 69:316–325
Mischke S, Sun Z, Herzschuh U, Qiao Z, Sun N (2010) An ostracod-inferred large Middle Pleistocene freshwater lake

in the presently hyper-arid Qaidam Basin (NW China). Quat Int 218:74–85

Murray AS, Wintle AG (2000) Luminescence dating of quartz using an improved single-aliquot regenerative-dose protocol. Rad Meas 32:57–73

Murray AS, Wintle AG (2003) The single aliquot regenerative dose protocol: potential for improvements in reliability. Rad Meas 37:377–381

Ning Y, Liu W, An Z (2009) A 130-ka reconstruction of precipitation on the Chinese Loess Plateau from organic carbon isotopes. Palaeogeogr Palaeoclimatol Palaeoecol 270:59–64

Owen LA, Finkel RC, Ma H, Barnard PL (2006) Late Quaternary landscape evolution in the Kunlun Mountains and Qaidam Basin, northern Tibet: a framework for examining the links between glaciation, lake level changes and alluvial fan formation. Quat Int 154–155:73–86

Prescott JR, Hutton JT (1994) Cosmic ray contributions to dose rates for luminescence and ESR dating: large depths and long-term time variations. Rad Meas 23:497–500

Rhode D, Ma H, Madsen DB, Brantingham PJ, Forman SL, Olsen JW (2010) Paleoenvironmental and archaeological investigations at Qinghai Lake, western China: geomorphic and chronometric evidence of lake level history. Quat Int 218:9–44

Roberts RM (2007) Assessing the effectiveness of the double-SAR protocol in isolating a luminescence signal dominated by quartz. Rad Meas 42:1627–1636

Shi Y, Yu G, Liu X, Li B, Yao T (2001) Reconstruction of the 30–40 ka BP enhanced Indian monsoon climate based on geological records from the Tibetan Plateau. Palaeogeogr Palaeoclimatol Palaeoecol 160:69–83

Sun YJ, Lai ZP, Long H, Liu XJ, Fan QS (2010) Quartz OSL dating of archaeological sites in Xiao Qaidam Lake of the NE Qinghai–Tibetan Plateau and its implications for palaeoenvironmental changes. Quat Geochron 5:360–364

Tian L, Masson-Delmotte V, Stievenard M, Yao T, Jouzel J (2001) Tibetan Plateau summer monsoon northward extent revealed by measurements of water stable isotopes. J Geophys Res 106:28081–28088

Vandenberghe J, Renssen H, van Huissteden K, Nugteren G, Konert M, Lu H, Dodonov A, Buylaert JP (2006) Penetration of Atlantic westerly winds into central and East Asia. Quat Sci Rev 25:2380–2389

Wang E, Xu FY, Zhou JX, Wan J, Burchfiel BC (2006) Eastward migration of the Qaidam basin and its implications for Cenozoic evolution of the Altyn Tagh fault and associated river systems. Geol Soc Am Bull 118:349–365

Wei X, Jiang J (1994) The evolution of the Quaternary salt lakes in the Qaidam Basin. Acta Geol Sin 7:71–82

Wünnemann B, Hartmann K, Janssen M, Zhang HC (2007) Responses of Chinese desert lakes to climate instability during the past 45,000 years. In: Madsen DB, Chen FH, Gao X (eds) Late Quaternary climate change and human adaptation in Arid China. Elsevier, Amsterdam, Developments in Quaternary Science 9, pp 11–24

Yang X, Scuderi LA (2010) Hydrological and climatic changes in deserts of China since the late Pleistocene. Quat Res 73:1–9

Yang B, Wang J, Shi Y, Braeuning A (2004) Evidence for a warm-humid climate in arid northwestern China during 40–30 ka BP. Quat Sci Rev 23:2537–2548

Yang X, Scuderi LA, Paillou C, Liu Z, Li H, Ren X (2011) Quaternary environmental changes in the drylands of China—a critical review. Quat Sci Rev 30:3219–3233

Yin A, Wang LC, Zhou SP, Chen XH, Gehrels GE, McRivette MW (2008) Cenozoic tectonic evolution of Qaidam basin and its surrounding regions (Part 1): the southern Qilian Shan-Nan Shan thrust belt and northern Qaidam basin. Geol Soc Am Bull 120:813–846

Yu G, Harrison SP, Xue B (2001) Lake status records from China: data base documentation. Max Planck Institute for Biogeochemistry, Technical Report #4. Jena

Zhang JR, Lai ZP, Jia YL (2012) Luminescence chronology for late Quaternary Lake levels of enclosed Huangqihai Lake in East Asian monsoon marginal area in northern China. Quat Geochron 10:123–128

Zheng MP, Xiang J, Wei XJ, Zheng Y (1989) Saline lakes on the Qinghai-Xizang (Tibet) Plateau. Beijing Scientific and Technical Publishing House, Beijing, pp 306–329 (in Chinese)

Zheng M, Meng Y, Wei L (2000) Evidence of the pan-lake stage in the period of 40–28 ka B.P. on the Qinghai-Tibet Plateau. Acta Geol Sinica 74:266–272